# Supplementary Information

## *ISPD* loss-of-function mutations disrupt dystroglycan *O*-mannosylation and cause Walker-Warburg syndrome

Tobias Willer, Hane Lee, Mark Lommel, Takako Yoshida-Moriguchi, Daniel Beltran Valero de Bernabe, David Venzke, Sebahattin Cirak, Harry Schachter, Jiri Vajsar, Thomas Voit, Francesco Muntoni, Andrea S. Loder, William B. Dobyns, Thomas L. Winder, Sabine Strahl, Katherine D. Mathews, Stanley F. Nelson, Steven A. Moore, Kevin P. Campbell*

* correspondence should be addressed to K.P.C.: kevin-campbell@uiowa.edu

# Supplementary Figure 1

**a**

| Genetic defect | WWS | MEB/FCMD | CMD | total | total % |
|---|---|---|---|---|---|
| ***POMT1*** | 8 | | 5 | 13 | 21% |
| ***POMT2*** | 1 | 6 | 5 | 12 | 19% |
| ***POMGnT1*** | 1 | 9 | 3 | 13 | 21% |
| ***FKTN*** | 1 | 4 | 3 | 8 | 13% |
| ***FKRP*** | 1 | | 4 | 5 | 8% |
| ***LARGE*** | | | 1 | 1 | 1% |
| **n.d.** | 11 (incl.7 *ISPD*) | | | 11 | 17% |
| **total** | 23 | 19 | 21 | 63 | 100% |
| **total %** | 37% | 30% | 33% | 100% | |

**b**

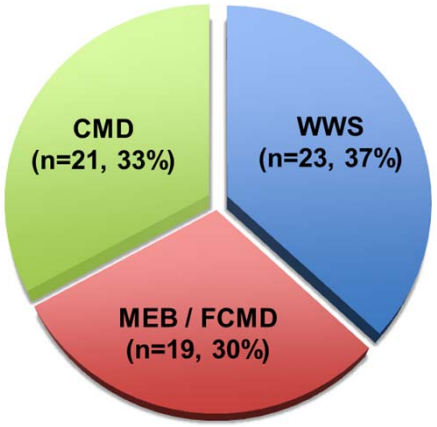


**c**

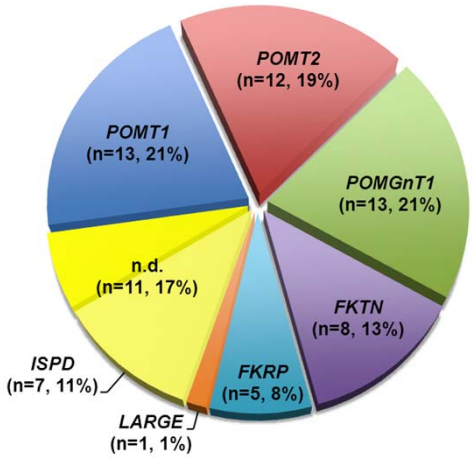


**Supplementary Figure 1. Genetic and phenotypic distribution of dystroglycanopathy patient fibroblasts analyzed by On-Cell western blot complementation**
(**a**) The table summarizes the On-Cell complementation assay results from 63 patient fibroblasts. Listed are the phenotypic distribution and mutation frequencies in each of the six glycosyltransferase genes within our patient cohort. (**b**) Pie chart representing the phenotypic distribution of patients analyzed by On-Cell complementation assay. (**c**) Pie chart representing the mutation frequencies in the patients analyzed by On-Cell complementation assay. The mutation frequencies of each candidate gene roughly correlate with previously published data by Godfrey *et al.* (2007)[1].

# Supplementary Figure 2

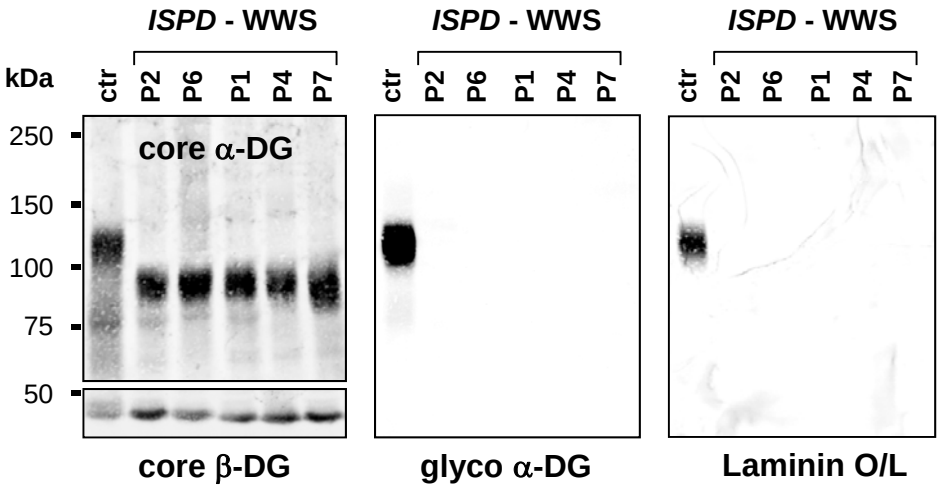


**Supplementary Figure 2. Western blot with WGA enriched glycoproteins from five WWS patients in complementation group 1**
Comparison of fibroblast α-DG glycosylation status reveals complete loss of functional α-DG glycosylation and a comparable hypoglycosylation of core α-DG in all patient samples. Immunoblot was probed with antibodies against the glycosylated form of α-DG (IIH6), core α-DG (G6317), and β-DG (AP83) as loading control. Receptor binding activity was analyzed with Laminin binding overlay assay.

# Supplementary Figure 3

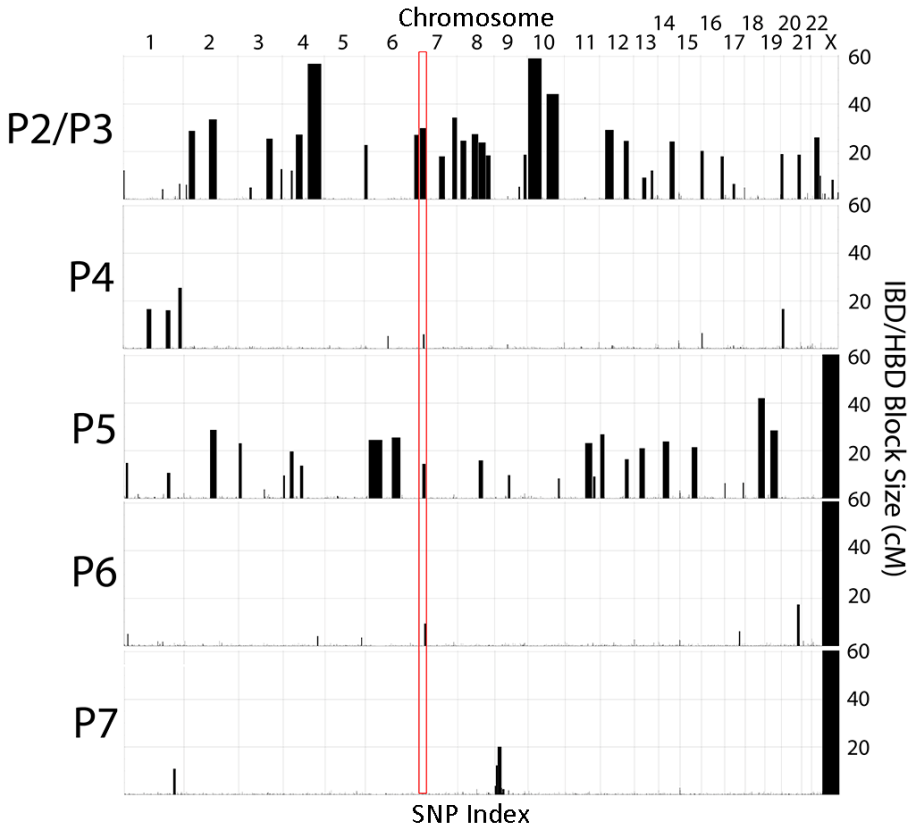


**Supplementary Figure 3. Alignment of identical-by-descent (IBD) and homozygosity-by-descent (HBD) intervals among *ISPD* deficient patients.** IBD or HBD block size is plotted according to cM along the y-axis, and according to SNP index along the x-axis. The ratio of the width of the block to the height of the block indicates the SNP density (# of SNPs/cM) within the interval. A region on chromosome 7 where three out of four suspected consanguineous samples are homozygous while overlapping with the P2/P3 Z2 region is highlighted by a red box.

# Supplementary Figure 4

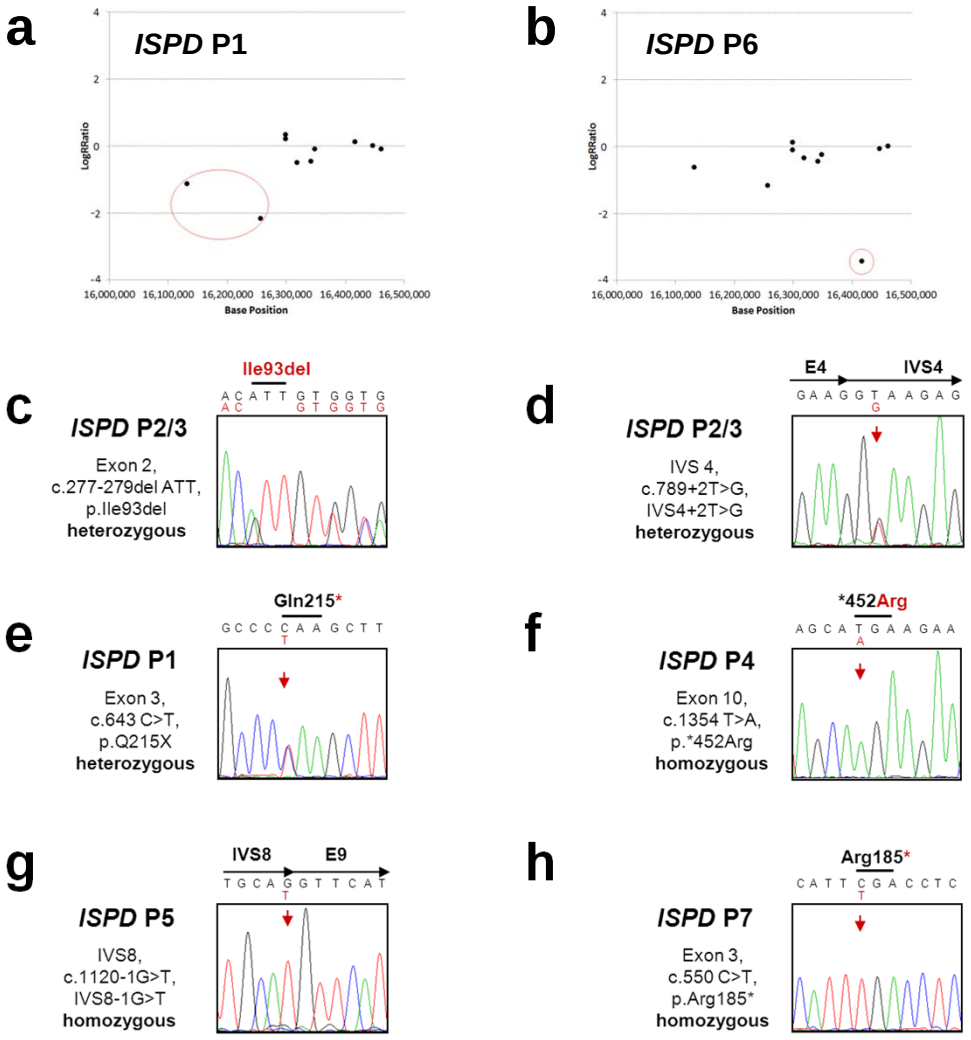


**Supplementary Figure 4. Genomic sequence analysis of *ISPD* deficient patients** LogRratio (LRR) reveals large exonic deletions in *ISPD* P1 and *ISPD* P6. The deletions were supported by the Illumina Omni-1 genotyping data. (**a**) *ISPD* P1: 53 contiguous SNPs spanning the two exons were all homozygous. The most outward boundaries of this heterozygous deletion were determined by the flanking SNPs of the 53 homozygous SNPs (rs1528149 and rs9918580), predicting the deletion could be up to 190 kb in size. (**b**) *ISPD* P6: Three SNPs near exon 3 (rs12699786, rs12671637, rs10237809) were not called while these SNPs were called with high confidence in the other 7 samples. The most outward boundaries of this homozygous deletion were determined by the flanking SNPs of the 3 SNPs not called (rs7789712 and rs11972185). (**c-g**) Sanger sequencing of *ISPD* deficient patients. Chromatograms with genomic DNA sequence variations are shown for *ISPD* patients P2/3 (**c,d**), P1 (**e**), P4 (**f**), P5 (**g**) and P7 (**h**).

# Supplementary Figure 5

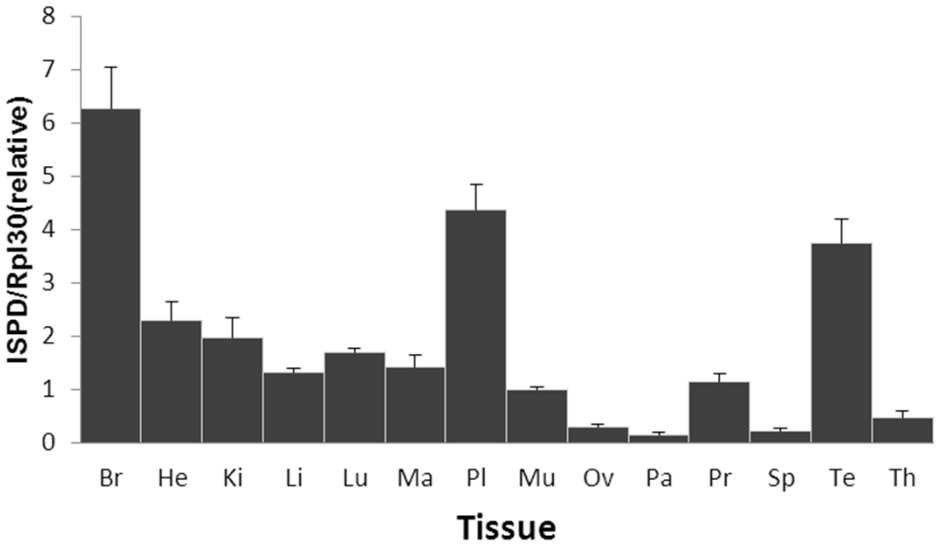


**Supplementary Figure 5. qPCR expression analysis of *ISPD* in human tissues**
*ISPD* shows ubiquitous expression in all tissues analyzed. Highest *ISPD* expression was detected in brain. For normalization ribosomal protein Rpl30 was used. Analyzed tissues: Br (brain), He (heart), Ki (kidney), Li (liver), Lu (lung), Ma (mammary gland), Pl (placenta), Mu (skeletal muscle), Ov (ovary), Pa (pancreas), Pr (prostate), Sp (spleen), Te (testis), Th (thymus)

# Supplementary Figure 6

**a**

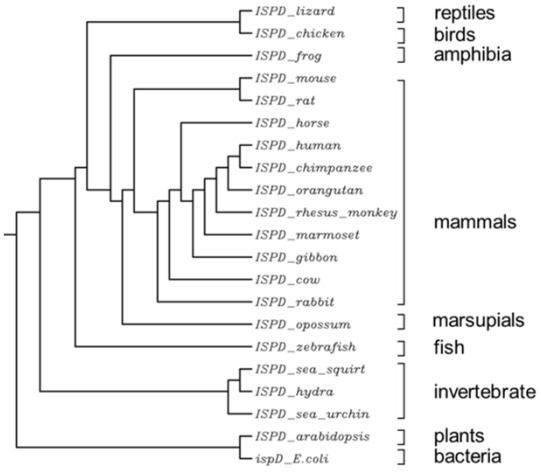


**b**

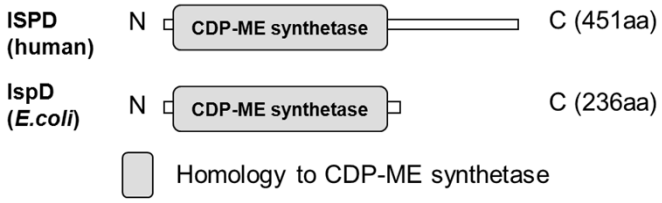


**c**

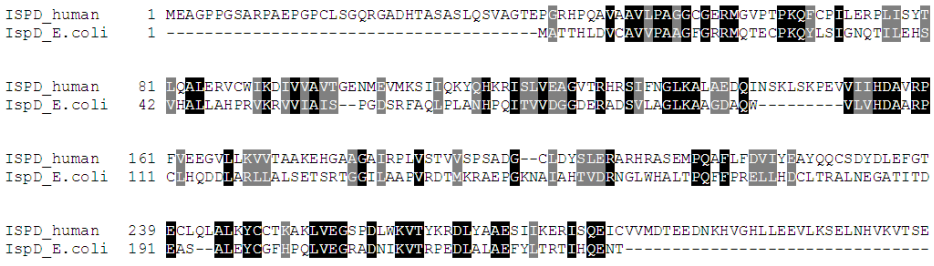


**Supplementary Figure 6. ISPD conservation across species**
(**a**) Phylogenic tree of ISPD proteins from different species. ISPD proteins are conserved from men to bacteria. Interestingly, no ISPD homologs are present in flies *(Drosophila melanogaster)* and nematodes *(Caenorhabditis elegans).* The dendrogram was generated using ClustalW sequence alignment. (**b**) Schematic representation of human and *E.coli* ISPD proteins. The shared proposed CDP-ME synthase catalytic domain is highlighted with a grey box. (**c**) Protein sequence alignment of protein ISPD sequences from human and *E.coli*. Both proteins sequence share 26% identity and 44% similarity. Identical amino acids are highlighted in black and similar amino acids are highlighted in grey.

# Supplementary Figure 7

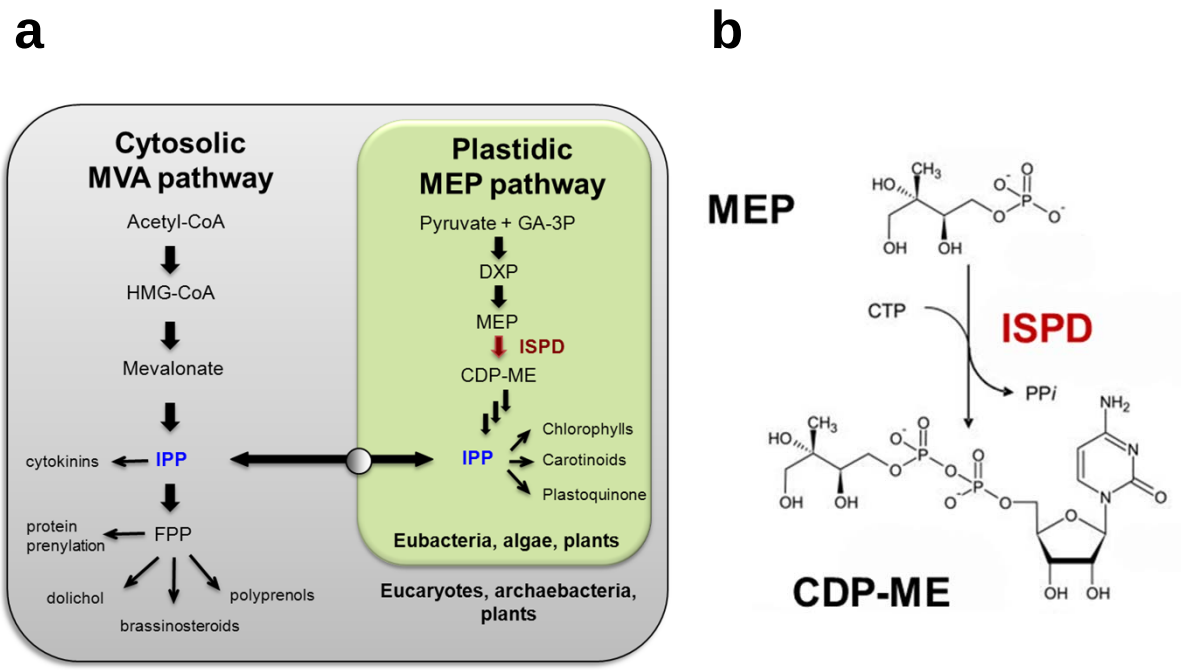


**Supplementary Figure 7. ISPD is involved in the MEP pathway for isoprenoid precursor synthesis**
(**a**) Schematic representation of the isoprenoid precursor synthesis which differs in human, plant and bacteria (adapted from Rodríguez-Concepción and Boronat, 2002)[2] . Mammals only use the MVA pathway, bacteria only use the MEP pathway, while plants use both pathways spatially separated in the cytoplasm and plastids. In plants both pathways are interconnected through the intermediate IPP (isopentenyl diphosphate, highlighted in blue). The biosynthetic step catalyzed by ISPD is highlighted in red.
(**b**) 4-diphosphocytidyl-2-C-methyl-D-erythritol synthase (ISPD) catalyzes the formation of 4-diphosphocytidyl-2-C-methyl-D-erythritol (CDP-ME) from 2-C-methyl-D-erythritol 4-phosphate (MEP) and CTP.

# Supplementary Figure 8

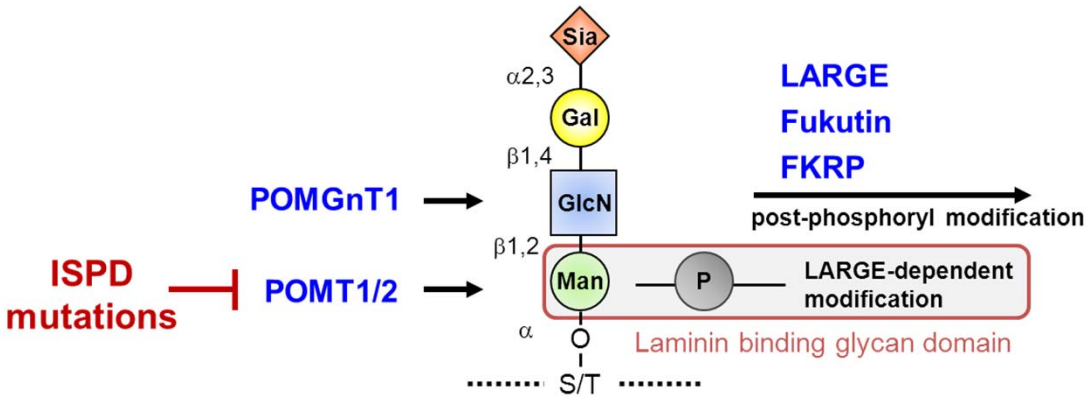


**Supplementary Figure 8. ISPD mutations impair protein *O*-mannosylation resulting in loss of laminin binding glycan**
Schematic representation of the α-DG functional glycan and the known WWS gene products (indicated in blue) that are involved in its synthesis. ISPD defects impair protein *O*-mannosylation, which is the initial step in the synthesis of the laminin binding glycan. LARGE, Fukutin and FKRP are postulated to be involved in the post-phoshoryl modification.

# Supplementary Table 1

| Mutant gene | Clinical phenotype | Zygosity | Nucleotide variant | Amino acid | Reference |
|---|---|---|---|---|---|
| **Control** | n.d. | | | | CRL-2127 (ATCC) |
| ***POMT1*** | WWS | heterozygous | c.997C>T<br>c.1006T>G | p.Pro273Leu<br>p.Leu276Arg | |
| ***POMT1*** | CMD | heterozygous | c.85A>C<br>c.1864C>T | p.Ser29Arg<br>p.Arg622* | |
| ***POMT1*** | LGMD | heterozygous | c.512T>G<br>genomic deletion of exon 18-19 | p.Leu171Arg<br>p.Ala589Val fs*38 | [3] |
| ***POMT2*** | WWS/MEB | heterozygous | c.1116+1G>A<br>c.1997A>G | p.Gln372fs<br>p.Tyr666Cyc. | |
| ***POMGnT1*** | WWS/MEB | heterozygous | c.794G>A<br>c.932G>A | p.Arg265His<br>p.Arg311Gln | |
| ***FKTN*** | WWS | heterozygous | c.385delA<br>c.1176C>A | p.Ile129fs*1<br>p.Tyr392* | GM16192 (Coriell Cell Repository) |
| ***FKRP*** | WWS | homozygous | c.1A>G | p.Met1Val | [4] |
| ***LARGE*** | CMD | homozygous | large intra-chromosomal duplication inserted into intron 10 | | [5] |

**Supplementary Table 1. Summary of control and dystroglycanopathy patient fibroblast cell lines**

# Supplementary Table 2

| Patient | Phenotype | Life span | α-DG functional glycosylation | Muscle | Brain | Eye | Reference |
|---|---|---|---|---|---|---|---|
| **P1** | WWS | 15 months | IIH6 negative | biopsy at 12 months dystrophic, CK 3,000 to 13,000 U/l | MRI at 3 days and 5 months: hydrocephalus, cobblestone lissencephaly, beaded subcortical heterotopia, thin corpus callosum, increased white matter signal, brainstem hypoplasia, cerebellar hypoplasia | bilateral microphthalmia and cataracts, arrested retinal development | |
| **P2** | WWS | 16 months | IIH6 negative | no biopsy, CK 5,400 U/l | MRI at 1 day: hydrocephalus with marked thinning of cortex, cobblestone lissencephaly, brain stem atrophy | bilateral microphthalmia with cataract, persistent hyperplastic primary vitreous, retinal detachment | |
| **P3** | WWS | 24 months | IIH6 negative | no biopsy, CK 3,300 U/l | MRI at 1 day: massive hydrocephalus, cerebellar hypoplasia, cobblestone lissencephaly | bilateral optic nerve hypoplasia, loss of macular pigment | |
| **P4** | WWS | unknown | IIH6 negative | unknown | unknown | unknown | Case #1980, Miami Brain and Tissue Bank for Developmental Disorders |
| **P5** | WWS | 6 months | IIH6 negative | biopsy at 1 month dystrophic, CK 2,927 U/l | MRI and autopsy: hydrocephalus, agyria, cobblestone lissencephaly, beaded subcortical heterotopia, thin corpus callosum, brainstem hypoplasia, cerebellar hypoplasia | unilateral microphthalmia with cataract, optic nerve hypoplasia | Case #1001, Miami Brain and Tissue Bank for Developmental Disorders[6,7] |
| **P6** | WWS | 3 months | IIH6 negative | dystrophic, CK 9,577 U/l | MRI and autopsy: hydrocephalus, agyria/pachygyria, cobblestone lissencephaly, cerebellar hypoplasia | Peters' anomaly, retinal detachment, cornea dysplasia | [8,9] |
| **P7** | WWS | unknown | IIH6 negative | dystrophic, CK 6,126 U/l | MRI: cobblestone lissencephaly with partial pachygyria, hydrocephalus, partial agenesis of corpus callosum, brainstem hypoplasia, cerebellar hypoplasia | unilateral congenital cataract, focal corneal clouding | |

**Supplementary Table 2. Clinical characteristics of *ISPD* deficient WWS cases**

# Supplementary Table 3

| Chromosome | Intervals targeted for sequencing (b37) | No. of families HBD/IBD at the interval | No. exons targeted |
|---|---|---|---|
| chr2 | 110,443,753-142,636,523 | 2 | 1,766 |
| chr4 | 114,226,988-131,107,545 | 2 | 600 |
| chr4 | 157,486,220-163,245,174 | 2 | 176 |
| chr4 | 25,531,234-35,429,711 | 2 | 202 |
| chr4 | 71,520,178-86,932,486 | 2 | 1,027 |
| chr7 | 15,066,544-18,938,376 | 4 | 157 |
| chr8 | 70,942,229-72,095,586 | 2 | 66 |
| chr8 | 84,739,785-103,732,048 | 2 | 1,029 |
| chr9 | 130,884,753-131,640,165 | 2 | 249 |
| chr10 | 112,562,802-119,178,574 | 2 | 556 |
| chr12 | 100,576,725-104,925,884 | 2 | 415 |
| chr16 | 3,301,360-6,149,092 | 2 | 498 |
| chr20 | 4,195,591-7,256,082 | 2 | 154 |
| chr20 | 53,875,809-57,914,046 | 2 | 218 |

**Supplementary Table 3. List of all targeted intervals for sequencing and the number of families that were HBD or IBD and the number of exons targeted at each interval are shown.**

# Supplementary Table 4

| Number of Variants | Gene symbol | Gene name | Process involved according to Gene Ontology Annotation Database |
|---|---|---|---|
| 4 | ***ISPD*** | isoprenoid synthase domain containing | isoprenoid biosynthetic process |
| 3 | ***PABPC1*** | Polyadenylate-binding protein 1 | RNA metabolic process |
| 3 | ***LRP1B*** | Low-density lipoprotein receptor-related protein 1B | protein transport, receptor-mediated endocytosis |
| 2 | ***SCTR*** | secretin receptor | G-protein coupled receptor signaling pathway |
| 2 | ***THSD7B*** | thrombospondin, type I, domain containing 7B | biological process unknown |
| 2 | ***POP1*** | processing of precursor 1, ribonuclease P/MRP subunit | RNA processing |

**Supplementary Table 4. Genes with multiple functional variants that PASSed the hard-filtration in the targeted sequencing data**

# Supplementary Table 5

| primer | sequence | comment |
|---|---|---|
| **7717** | 5'-ATGgaggccgggccgccgg-3' | forward primer, start ATG is capitalized |
| **7718** | 5'-**cta**CAAGTCTTCTTCAGAAATAAGTTTTTGTTC gctagcccctgctatcagaagctgaccaatg-3' | reverse primer, myc-tag is capitalized, STOP codon is highlighted in bold |

**Supplementary Table 5. Primers for human *ISPD* cloning**

# Supplementary Table 6

## a

| | | | P1 | P2 | P3 | P4 | P5 | P6 | P7 |
|---|---|---|---|---|---|---|---|---|---|
| **SNV** | No of variants | All | 684 | 688 | 689 | 667 | 567 | 670 | 674 |
| | | Known* | 669 | 667 | 668 | 637 | 555 | 647 | 656 |
| | | Novel† | 15 | 21 | 21 | 30 | 12 | 23 | 18 |
| | | dbSNP132_rate (%) | 97.807 | 96.948 | 96.952 | 95.502 | 97.884 | 96.567 | 97.329 |
| | | Concordance_rate (%)‡ | 99.701 | 99.550 | 99.551 | 99.686 | 99.640 | 99.845 | 99.695 |
| | Het/Homo Ratio | All | 1.581 | 1.520 | 1.487 | 1.027 | 1.054 | 1.680 | 1.832 |
| | | Known | 1.525 | 1.443 | 1.412 | 0.942 | 1.026 | 1.609 | 1.756 |
| | | Novel | 15.000 | 21.000 | 21.000 | 29.000 | 5.000 | 10.500 | 18.000 |
| | Ti/Tv Ratio | All | 3.329 | 2.909 | 2.915 | 3.018 | 3.050 | 2.941 | 2.965 |
| | | Known | 3.344 | 2.947 | 2.953 | 3.057 | 3.081 | 2.969 | 2.952 |
| | | Novel | 2.750 | 2.000 | 2.000 | 2.333 | 2.000 | 2.286 | 3.500 |
| **INDEL** | No of variants | All | 55 | 50 | 44 | 56 | 52 | 58 | 56 |
| | | Known | 11 | 10 | 11 | 11 | 11 | 11 | 12 |
| | | Novel | 44 | 40 | 33 | 45 | 41 | 47 | 44 |
| | | dbSNP132_rate (%) | 0.200 | 0.200 | 0.250 | 0.196 | 0.212 | 0.190 | 0.214 |
| | Het/Homo Ratio | All | 1.500 | 0.923 | 0.760 | 0.867 | 0.529 | 1.148 | 1.154 |
| | | Known | 0.833 | 0.667 | 0.571 | 0.833 | 0.833 | 0.833 | 2.000 |
| | | Novel | 1.750 | 1.000 | 0.833 | 0.875 | 0.464 | 1.238 | 1.000 |

* known: dbSNP132 positions
† novel: not dbSNP132 positions
‡ concordance rate (%): the rate of the known SNPs with the same genotype as in the dbSNP132

## b

| | | P1 | P2 | P3 | P4 | P5 | P6 | P7 |
|---|---|---|---|---|---|---|---|---|
| **SNV** | total | 15 | 21 | 21 | 30 | 12 | 23 | 18 |
| | missense | 7 | 9 | 9 | 14 | 6 | 12 | 10 |
| | nonsense | 1 | 0 | 0 | 1 | 0 | 0 | 1 |
| | splice-5 | 0 | 1 | 1 | 0 | 0 | 0 | 0 |
| | splice-3 | 0 | 0 | 0 | 0 | 0 | 0 | 0 |
| | Others* | 7 | 11 | 11 | 15 | 6 | 11 | 7 |
| **INDEL** | total | 44 | 40 | 33 | 45 | 41 | 47 | 44 |
| | frameshift | 2 | 4 | 3 | 3 | 2 | 4 | 4 |
| | coding | 3 | 4 | 4 | 4 | 2 | 5 | 4 |
| | others† | 39 | 32 | 26 | 38 | 37 | 38 | 36 |

* others: SNPs found in the 1000 Genome database or dbSNP131 outside the coding-region and coding-synonymous SNPs
† others: INDELs found in the 1000 Genome database or dbSNP131 or outside the coding-region

**Supplementary Table 6. Summary statistics of variant analyis**
(**a**) Summary Statistics of the Variants Called and PASSed Filters
(**b**) Summary Statistics of the Novel Variants Called and PASSed Filters

**References for Supplemental Information**


1. Godfrey, C. *et al.* Refining genotype phenotype correlations in muscular dystrophies with defective glycosylation of dystroglycan. *Brain : a journal of neurology* **130**, 2725-35 (2007).
2. Rodriguez-Concepcion, M. & Boronat, A. Elucidation of the methylerythritol phosphate pathway for isoprenoid biosynthesis in bacteria and plastids. A metabolic milestone achieved through genomics. *Plant physiology* **130**, 1079-89 (2002).
3. Lommel, M. *et al.* Correlation of enzyme activity and clinical phenotype in POMT1-associated dystroglycanopathies. *Neurology* **74**, 157-64 (2010).
4. Van Reeuwijk, J. *et al.* A homozygous FKRP start codon mutation is associated with Walker-Warburg syndrome, the severe end of the clinical spectrum. *Clinical genetics* **78**, 275-81 (2010).
5. Clarke, N.F. *et al.* Congenital muscular dystrophy type 1D (MDC1D) due to a large intragenic insertion/deletion, involving intron 10 of the LARGE gene. *European journal of human genetics : EJHG* **19**, 452-7 (2011).
6. Satz, J.S. *et al.* Brain and eye malformations resembling Walker-Warburg syndrome are recapitulated in mice by dystroglycan deletion in the epiblast. *The Journal of neuroscience : the official journal of the Society for Neuroscience* **28**, 10567-75 (2008).
7. Kanoff, R.J. *et al.* Walker-Warburg syndrome: neurologic features and muscle membrane structure. *Pediatric neurology* **18**, 76-80 (1998).
8. Vajsar, J., Ackerley, C., Chitayat, D. & Becker, L.E. Basal lamina abnormality in the skeletal muscle of Walker-Warburg syndrome. *Pediatric neurology* **22**, 139-43 (2000).
9. Chitayat, D. *et al.* Prenatal diagnosis of retinal nonattachment in the Walker-Warburg syndrome. *American journal of medical genetics* **56**, 351-8 (1995).